Dual Boundary Element Applied to 2D Fatigue Crack Propagation in a Thin Aluminum Plate

Marcel Sato, msato@fem.unicamp.br
Paulo Sollero, sollero@fem.unicamp.br
Éder Lima de Albuquerque, ederlima@fem.unicamp.br
Renan Rodrigues de Mello Ozelo, renanozelo@fem.unicamp.br
Universidade Estadual de Campinas UNICAMP - R. Mendeleiev, 200, Campinas, 13083-970, SP, Brasil

Abstract. *In this paper a general procedure for the analysis of two-dimensional multiple site fatigue crack propagation is presented. The crack propagation is simulated using an incremental crack extension procedure based on the strain energy density criterion and the Paris law. The dual boundary element method is used to perform a single region stress/strain analysis of the cracked specimen. Stress intensity factors are evaluated using the J-Integral technique and they are decoupled using a procedure based on the decomposition of the elastic field into its symmetric and anti-symmetric mode components. Crack extensions are automatically modeled with the introduction of new boundary elements along the crack fronts. This procedure is applied to the analysis of a thin cracked plate made of 2024-T3 aluminum alloy under cyclic loading and the results are compared with experimental data.*

Keywords*: Boundary Element Method, Fatigue, Crack Propagation*

1. INTRODUCTION

In engineering applications, the problem of fatigue crack propagation is one of the most important to be taken into account in the design of the product. The professional needs to estimate an operation life for the component such as a number of cyclic loads or fatigue cycles, where one can ensure that the component is not going to fail in a catastrophic manner. The presence of cracks in engineering structures is practically impossible to be avoided and, up to a certain size, they are acceptable with some security.

The complexity of the engineering projects have increased along the time and good alternatives need to be found in order to reduce the number of experimental tests required to validate a product or device. In this context, the numerical simulations play a fundamental role in the field of engineering and technology.

In this work, a fatigue crack propagation analysis is performed in a mixed-mode problem using an algorithm based on a Dual Boundary Element Method. The results provided by this code are compared with those obtained through experimental tests of the specimens and are in good agreement.

2. DUAL BOUNDARY ELEMENT METHOD

The Boundary Element Method (BEM) is a well-established numerical technique in engineering, as reported by Brebbia and Dominguez (1992). However, the solution of general problems involving cracks in the structure cannot be achieved with the direct application of the BEM in a single region formulation, because the coincidence of the crack surfaces generates identical boundary integral equations which lead to an ill-conditioned numerical problem. A special formulation of this method applied to fracture problems can overcome this problem is known as Dual Boundary Element Method (DBEM), and was proposed by Portela (1992a, 1992b). This method incorporates two independent boundary integral equations, with the displacement equation applied to one of the crack surfaces and the traction equation on the other. These equations are defined as

$$c_{ij}(x')\,u_j(x')+\int_{\Gamma} t^*_{ij}(x',x)\,u_j(x)\,d\Gamma(x)=\int_{\Gamma} u^*_{ij}(x',x)\,t_j(x)\,d\Gamma(x) \tag{1}$$

and

$$\frac{1}{2}t_j(x')+n_i(x')\int_{\Gamma} S_{kij}(x',x)\,u_k(x)\,d\Gamma(x)=n_i(x')\int_{\Gamma} D_{kij}(x',x)\,t_k(x)\,d\Gamma(x)\ , \tag{2}$$

where i and j denote the Cartesian coordinates; c_{ij} is given by $\delta_{ij}/2$ for smooth surfaces (δ_{ij} is the Kronecker delta); u_j is the displacement field; t_j is the traction vector; n_i is the component of the normal vector in the direction i; S_{kij} and D_{kij} are the derivatives of the fundamental solutions; Γ denotes the geometry boundary; x and x' are the field and source points, respectively; the distance between x and x' is denoted by r; u_{ij}^* and t_{ij}^* denote the fundamental solutions for displacements and tractions, respectively. The expressions for the fundamental solutions and their derivatives can be found in the literature, see Brebbia and Dominguez (1992).

Applying Eq. (1) on one of the crack surfaces and Eq. (2) on the other, is possible to overcome the problem of coincident points and the crack problem can be solved in a single region analysis. This feature is interesting to threat crack propagation problems in incremental analysis, because the increments are created with a simple procedure. In this situation, the increment is modeled with the introduction of new boundary elements without the necessity of remeshing the entire boundary.

In order to model this problem, a simple strategy is adopted. The discretization of the crack boundaries is made with discontinuous elements (that satisfy continuity and smoothness requirements) and the boundary integral equations shown in Eq. (1) and Eq. (2) are applied for the upper and lower boundaries, respectively. The discretization of the other boundaries of the geometry is made with continuous elements and the displacement boundary integral equation.

3. FATIGUE CRACK PROPAGATION ANALYSIS

Structures with cracks under cyclic loads are very common. The cyclic loading can lead to an increase in the crack length trough the service time and it can be a problem if the crack reaches a certain critical length. Applying concepts of the Linear Elastic Fracture Mechanics (LEFM) is possible to overcome the problem of fatigue crack propagation of several applications through numerical analysis.

3.1. Stress Intensity Factor Computation

The stress intensity factor is the main parameter of the LEFM and is related to the deformation mode of the solid so that, for the case of a two dimensional problem, there are two stress intensity factors denoted by K_I and K_{II}. There are some ways to evaluate these parameters and the J-Integral is the technique chosen in this work. The J-Integral is path independent and its application to the fracture mechanics was first proposed by Rice (1968). For a two dimensional case, this integral is given by

$$J = \int_{\Gamma} \left(W n_1 - t_j u_{j'1} \right) ds \,, \tag{3}$$

where Γ denotes an arbitrary path surrounding the crack tip which is integrated in the anti-clockwise sense; W is the strain energy density; t_j are the tractions and n_1 is the component in the direction 1 of the normal vector. Figure 1 shows a geometric model to evaluate this integral.

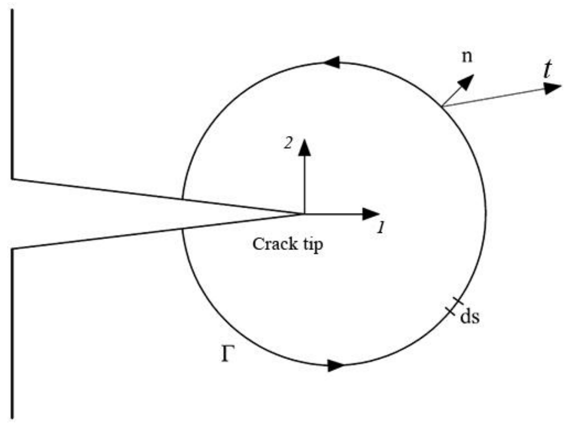

Figure 1. Geometric model to evaluate the J-Integral.

In the context of the LEFM this integral provides the same value of the energy release rate G, so that, one can suggest the following relation between this integral value and the stress intensity factors:

$$J = \frac{K_I^2 + K_{II}^2}{E'} \tag{4}$$

where $E' = E$ for plane stress and $E' = E/(1-\nu^2)$ for plane strain conditions. In these relations, υ is the Poisson's ratio.

It is possible to see from the Eq. (4) that the stress intensity factors need to be decoupled in a way one can rewrite it as $J = J^I + J^{II}$ where the superscript denotes the deformation modes. A simple procedure based on the decomposition of the elastic field into its symmetric and anti-symmetric mode components is used to decouple this relation. This procedure was proposed by Bui (1983) and can be found in the recent literature, see Aliabadi (2002). With the decoupled components, Eq. (3) becomes

$$J^m = \int_{\Gamma} \left(W^m n_1 - t_j^m u_{j'1}^m \right) ds \,, \tag{5}$$

where m denotes the mode component (it does not indicate summation). From Eq. (4) and Eq. (5) is possible to write the following relations:

$$J^I = \frac{K_I^2}{E'} \tag{6}$$

$$J^{II} = \frac{K_{II}^2}{E'} \tag{7}$$

So, from the Eq. (6) and Eq. (7) is possible to estimate the stress intensity factors K_I and K_{II} from the result provided by the application of the J-Integral technique. In this work, the integration of the Eq. (5) is performed by the Simpson's rule with good results.

3.2. Crack Growth Direction

There are many criteria in the literature to evaluate the direction of the crack increment in an incremental fatigue crack propagation analysis. One of the most used is the Minimum Strain Energy Density Criterion (MSED) or S-criterion that was proposed by Sih (1973a, 1973b). It states that the crack propagation direction coincides with the position where the minimum density energy factor is present, considering a region located with a distance r far from the crack tip. The density energy factor is obtained through the stress intensity factors evaluated at the crack tip, and can be written for a two dimensional context as

$$S = a_{11} K_I^2 + 2 a_{12} K_I K_{II} + a_{22} K_{II}^2 \;, \tag{8}$$

where

$$a_{11} = \frac{1}{16\mu} \left[1 + cos(\theta) \right] \left[\kappa - cos(\theta) \right] , \tag{9}$$

$$a_{12} = \frac{1}{16\mu} sin(\theta) \left[2cos(\theta) - (\kappa - 1) \right] , \tag{10}$$

$$a_{22} = \frac{1}{16\mu} \left\{ (\kappa + 1) \left[1 - cos(\theta) \right] + \left[1 + cos(\theta) \right] \left[3cos(\theta) - 1 \right] \right\} . \tag{11}$$

In these equations, μ is the shear modulus of the material; θ is the crack propagation angle in the system coordinates located at the crack tip and $\kappa = 3 - 4\nu$, for plane strain, or $\kappa = 3 - \nu/1 + \nu$, for plane stress.

In order to obtain the minimum value of the S, the expression in Eq. (8) is derived twice. The second derivative of this expression needs to be positive in order to satisfy the condition of minimum. These derivatives are showed below:

$$\begin{aligned} &\left[2\cos(\theta) - (\kappa - 1) \right] \sin(\theta) K_I^2 + 2 K_I K_{II} \left[2\cos(2\theta) - (\kappa - 1)\cos(\theta) \right] + \\ &+ K_{II}^2 \left\{ \left[\kappa - 1 - 6\cos(\theta) \right] \sin(\theta) \right\} = 0 \end{aligned} \tag{12}$$

$$K_I^2\left[2\cos(2\theta)-(\kappa-1)\cos(\theta)\right]+2K_IK_{II}\left[(\kappa-1)\sin(\theta)-4\sin(2\theta)\right]+$$
$$+K_{II}^2\left[(\kappa-1)\cos(\theta)-6\cos(2\theta)\right]>0 \tag{13}$$

Finding the angle from the Eq. (12) that satisfies the relation in Eq. (13), the problem of the crack increment direction is solved. The Bisection Method is a root finding algorithm simple and robust, so that, this method was used to solve Eq. (12) and it has been providing good results.

A special feature of this method is very useful for the evaluation of the increment size in an incremental crack propagation analysis. From the third hypothesis proposed by Sih (1973a, 1973b), which states that the ratio between *S* and Δa is constant through the propagation process, it is possible to obtain the next increment size as follows:

$$\Delta a_{i+1} = \frac{S_{i+1}}{S_i}\Delta a_i \, , \tag{14}$$

where Δa is the increment size; *i* and *i+1* represent the current and next increments, respectively.

3.3. Fatigue Life

There are many expressions to model the stable fatigue crack propagation that occur in the region II shown in the Fig. 2. The most used and known is the so-called "Paris Law" proposed by Paris and Erdogan (1960). The main drawback of this approach is that it does not consider the influence of the stress ratio, *R*, given by $R = K_{min}/K_{max}$. The expression of the Paris law is

$$\frac{da}{dN} = C\,\Delta K^m \, , \tag{15}$$

where *da/dN* is the crack growth rate; *C* and *m* are constants and ΔK is the range of the stress intensity factor given by $\Delta K = K_{max} - K_{min}$. The constants that appear in this relation are empirically determined and they depend on the load conditions, environment, type of material, etc. There are many researchers that proposed relations to model all the three regions from the Fig. 2, but these approaches are beyond the scope of the present work and they are not discussed here.

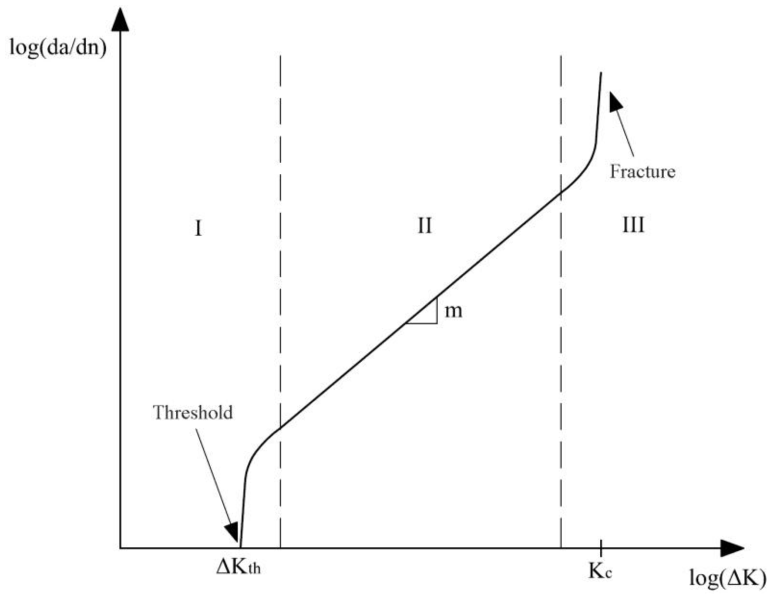

Figure 2. Typical fatigue crack growth behavior in metals.

3.3.1. Crack Closure

In many cases, the Paris law does not work very well due to the problem of the crack closure. The crack closure phenomenon was discovered by Elber (1970, 1971, 1976), by means of his experiments, when he noticed that the crack was not fully opened, even for loads substantially higher than zero. This was attributed to the compressive loads transmitted through the faces of an unloaded fatigue crack, caused by the plastic strains that surround the crack tip region, a phenomenon termed plasticity-induced fatigue crack closure (Meggiolaro and Castro, 2001). Figure 3 shows some schemes of mechanisms of closure. The roughness-induced closure is caused by the contact between the crack surfaces due to mode II deformations, which is a characteristic of mixed-mode problems. More details concerning to the fatigue crack closure problems are present in Cisilino and Aliabadi (2004).

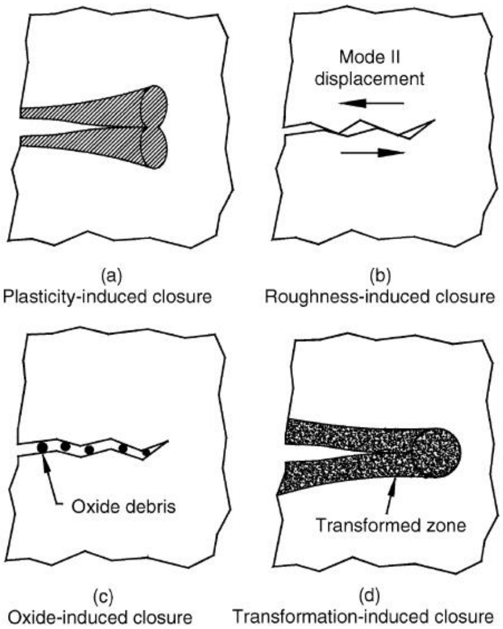

Figure 3. Fatigue crack closure mechanisms (Cisilino and Aliabadi, 2004).

Elber assumed that crack growth cannot take place under cyclic loads until the fatigue crack is fully opened and it would happen at a stress intensity factor $K_{op} > 0$. With this consideration the new stress intensity factor, now named as effective, is given by

$$\Delta K_{eff} = K_{max} - K_{op} \tag{16}$$

and now this is the fatigue crack propagation controlling parameter. The behavior of K during the test can be shown in the schematic diagram from Fig. 4.

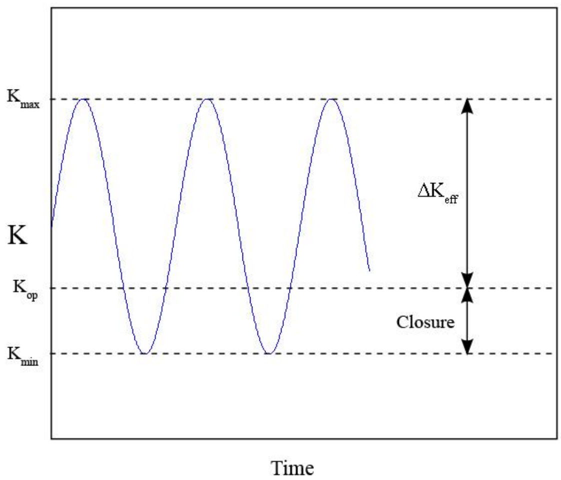

Figure 4. Stress intensity factor range and closure.

Using the considerations provided by the crack closure concept and the modified stress intensity factor range, it is possible to modify the Paris law to take into account this model. So, Elber proposed a modification in the Eq. (15):

$$\frac{da}{dN} = C\left(U\,\Delta K\right)^m , \tag{17}$$

where $U = \left(K_{max} - K_{op}\right)/\left(K_{max} - K_{min}\right)$.

In his work, Elber (1970, 1971) proposed a relation between the parameter U and the stress ratio, given by:

$$U = 0.5 + 0.4\,R , \tag{18}$$

for $-0.1 \le R \le 0.7$. Schijve (1981) proposed a modification of Eq. (18):

$$U = 0.55 + 0.33R + 0.12R^2 , \tag{19}$$

valid to $-1.0 \le R \le 0.54$. Eq. (18) and Eq. (19) were obtained to 2024-T3 aluminum alloy.

Using Eq. (17) instead of Eq. (15), one can obtain the number of cycles by the integration of this equation applying the trapezoidal rule. Using this procedure, the number of cycles is determined by

$$\Delta N = \frac{\left(a - a_0\right)}{2}\frac{1}{C}\left\{\frac{1}{\left[U\Delta K\left(a_0\right)\right]^m} + \frac{1}{\left[U\Delta K\left(a\right)\right]^m}\right\}, \tag{20}$$

where N is the number of fatigue cycles; $\left(a - a_0\right)$ is the increment advanced by the crack during the propagation; $\Delta K\left(a_0\right)$ and $\Delta K\left(a\right)$ are the range of the stress intensity factors evaluated in a_0 and a , respectively.

3.4. Incremental Analysis

The simulation of the crack propagation in the present work is made by means of an incremental analysis, where the crack increment is modeled with the introduction of new boundary elements in a simple procedure. This is possible, because of the intrinsic characteristic of the DBEM in the need of modeling only the boundaries of the geometry. Then, the simulation follows a systematic procedure: firstly, the problem is analyzed by the DBEM providing reliable results for the stress/strain fields. For each crack tip present in the structure, the J-Integral is applied for the computation of the stress intensity factors using the results from the elastic field, and the crack propagation angle is determined by means of the MSED. The crack increment size for the next incremental step is evaluated using the Eq. (14) and the number of cycles for the current incremental step is calculated through the Eq. (20). This procedure is repeated for all the crack tips. After that, the new increments are created by the introduction of new boundary elements into the structure and the system is updated. Again, the DBEM is used to perform a stress/strain analysis and the whole procedure is repeated until a limit number of increments or if the K_{Ic} (fracture toughness) is reached (the fracture toughness is the limit which separates the stable and unstable crack propagation). The algorithm implemented in this work uses this procedure and has provided good results.

4. EXAMPLE AND RESULTS

An example of the application of the crack propagation code is in the problem of a thin cracked plate made of 2024-T3 aluminum alloy subjected to a cyclic loading. The cracked plate has a notch inclined 45º, as shown in Fig. 5 (a), characterizing a mixed-mode fatigue crack propagation problem and a tension of 92.63 MPa is applied under a stress ratio of $R=0.0833$. This problem was simulated in an experimental work with a test frequency of 8 Hz for the pre-crack stage and for the effective fatigue test. This condition was achieved using a servo-hydraulic test machine. The pre-crack was 4 mm long for the two cracks that appeared in the notch tips (the pre-cracks were symmetric) of two plates tested. The crack propagation was monitored until it reached the length of 20 mm approximately for both cracks in the specimens. More details concerned to the experimental tests are going to be available in Sato (2009). Figure 5 (a) shows the geometry of the specimen used in the tests where it is possible to see the location of the notch at the center of the plate. The notch was machined through Electrical Discharge Machine (EDM) method. It is approximately 22 mm long and 0.4 mm wide. The plate thickness is 1.02 mm.

This problem was simulated using a simplified model based on the geometry shown in Fig. 5 (a). Only the rectangular region was modeled, discarding those regions with the presence of the holes and fillets (these regions were used to fix the plate in the machine). Figure 5 (b) shows the model used to simulate the problem where it is possible to see the discretization of the geometry, the presence of the pre-cracks and the assumed boundary conditions. A tension of 92.63 MPa was applied to the nodes at the lower boundary of the structure under a stress ratio of 0.0833 and the nodes at the upper boundary were constrained. In this model, 48 quadratic continuous elements were used to model the boundaries of the geometry and 70 quadratic discontinuous elements were used for the discretization of the pre-cracks and notch. During the propagation, new increments were modeled with 4 quadratic discontinuous elements. In the simulation, it was used 9 increments to reach the final configuration of the propagated path and Tab. 1 presents the increment lengths predicted by the algorithm where the upper crack is denoted by "*crack 1*" and the lower by "*crack 2*". The modulus of elasticity of the material is 73.1 GPa and the Poisson's ratio is 0.33. The constants C and m from the Paris law were assumed 1.42*e*-8 and 3.59, respectively (Sabelkin *et al.*, 2006). Figure 6 shows the propagated crack path obtained with the simulation and through the experimental tests, where it is possible to see the good agreement between the two results in a qualitative way.

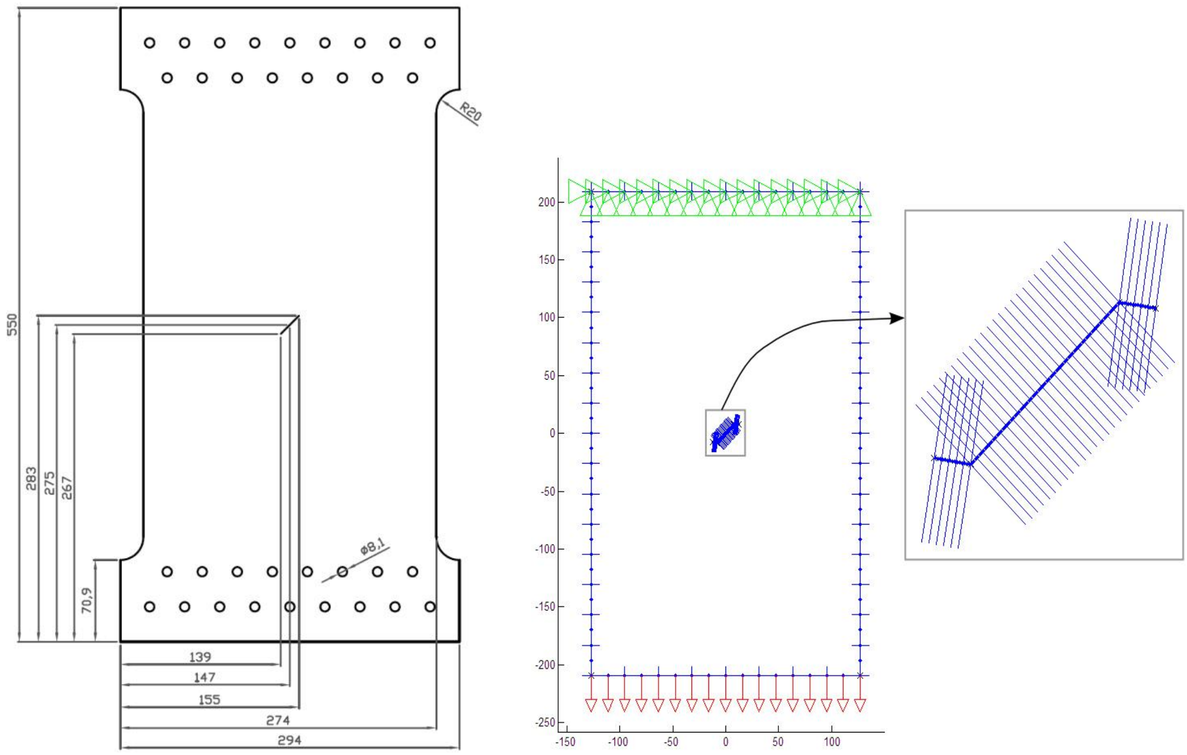

(a) (b)

Figure 5. (a) Geometry of the specimen tested (all dimensions are in mm). (b) Model used in the simulation.

Table 1. Increment lengths predicted by the algorithm for the simulation.

Increment	*Crack 1*	*Crack 2*
1	1.0000	1.0000
2	1.2632	1.2478
3	1.5107	1.5054
4	1.7701	1.7616
5	2.0510	2.0417
6	2.3624	2.3550
7	2.7228	2.7089
8	3.1363	3.1242
9	3.6277	3.6093

The values of the stress intensity factor K_I and K_{II} calculated by the algorithm during the propagation are shown in Tab. 2 and Tab. 3 for the *crack 1* and *crack 2*, respectively. Table 4 shows the angles predicted by the MSED criterion during the simulation.

Table 2. Values for K_I and K_{II} obtained during the propagation for *crack 1*.

Increment	K_I $\left[MPa\sqrt{m}\right]$	K_{II} $\left[MPa\sqrt{m}\right]$
1	19.0633	-0.7662

2	19.7049	0.4312
3	20.5065	-0.3290
4	21.4808	-0.1614
5	22.5864	0.1554
6	23.8139	-0.4719
7	25.2234	0.1460
8	26.7744	-0.3756
9	28.5413	0.1315

Table 3. Values for K_I and K_{II} obtained during the propagation for *crack 2*.

Increment	$K_I \left[MPa\sqrt{m}\right]$	$K_{II} \left[MPa\sqrt{m}\right]$
1	19.1092	0.7323
2	19.5845	-1.3933
3	20.5200	0.2155
4	21.4779	-0.2985
5	22.5881	-0.1440
6	23.8361	0.1536
7	25.2148	-0.4222
8	26.7871	0.1467
9	28.5330	-0.3628

Table 4. Angles predicted by the MSED criterion during the simulation
(According to the local system of coordinates at the crack tip).

Increment	*Crack 1*	*Crack 2*
1	4.5732	355.6370
2	357.4991	7.9396
3	1.8357	358.7977
4	0.8609	1.5905
5	359.2120	0.7303
6	2.2622	359.2619
7	359.3370	1.9130
8	1.6039	359.3728
9	359.4721	1.4541

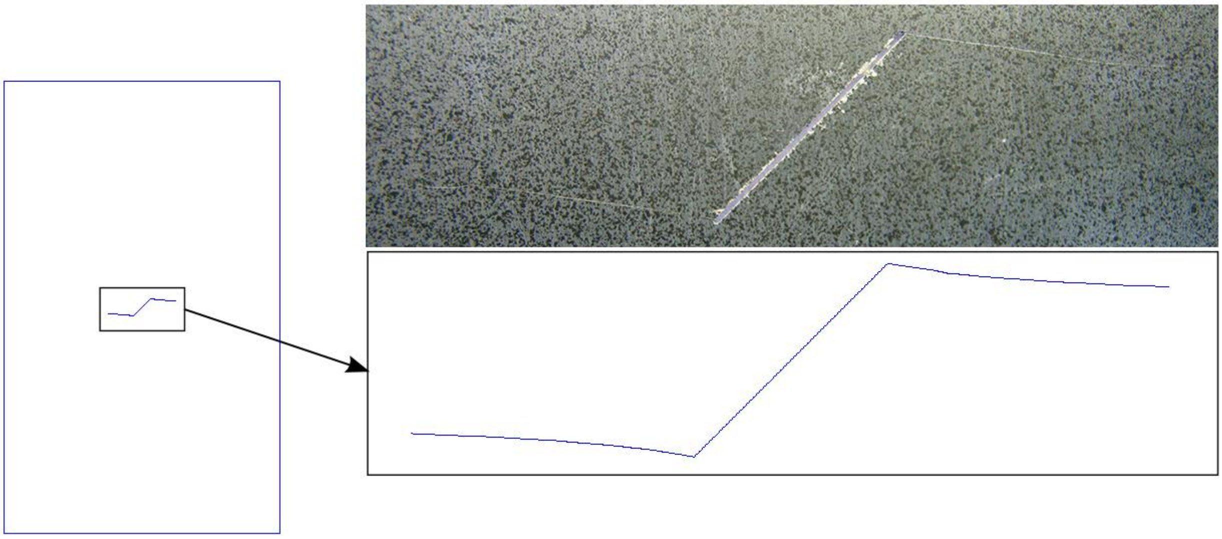

Figure 6. Propagated crack path obtained with the simulation (blue) and through experimental observation (picture).

The fatigue life was evaluated using the crack closure concept. But, neither Elber's model nor Schijve's were able to predict it with good precision. For this problem, Elber's model predicts $U = 0.5333$ while Schijve's model predicts $U = 0.5783$. It means that only 53.33% of the total stress intensity range is acting in the specimen for the Elber's model and only 57.83% of the total stress intensity range is acting in the specimen for the Schijve's model. Figure 7 shows the fatigue life curves predicted by each one of the models in comparison with the results for the *crack 1* of the first test specimen.

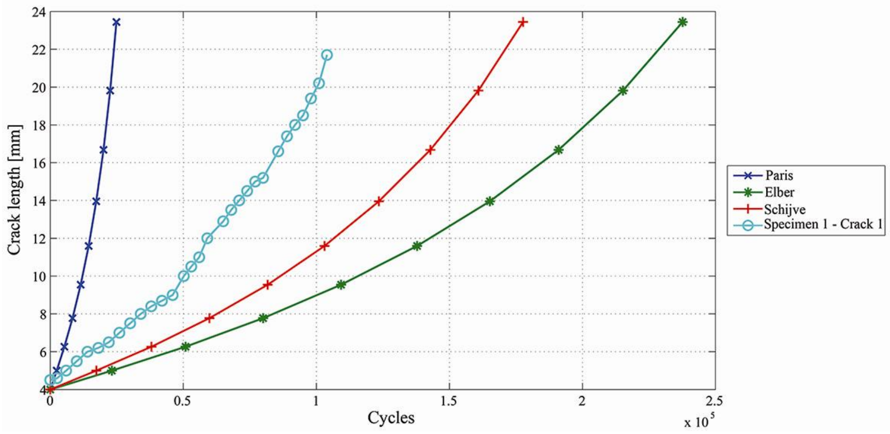

Figure 7. Comparison between the fatigue life curve predict by different models and experimental result for the *crack 1* of the first specimen tested.

From the observation of Fig. 7, it is clear that there is retardation in the fatigue life curve and it can be modeled using the crack closure model, but taking into account a higher value of the parameter U than that predicted by Schijve's model. In this work, the value of this parameter that best correlates the experimental and numerical curves is U=*0.66*. The crack closure model was chosen, and it is a reasonable tool for this situation because of the mixed-mode behavior of the crack propagation problem. Figure 8 shows the fatigue life curves for the *crack 1* obtained through the experimental tests of two specimens and numerically. Due to the symmetry of the two cracks, only one fatigue life curve is being shown.

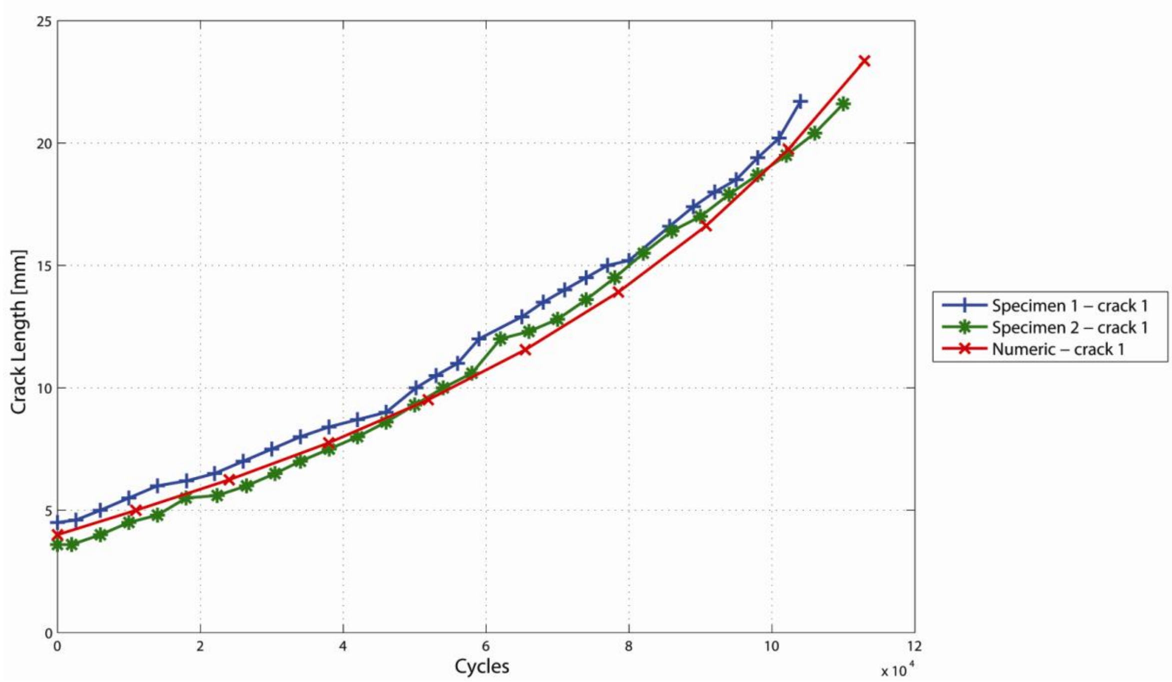

Figure 8. Fatigue life of *crack 1*. Comparison between experimental results for two specimens tested and numerical results.

5. CONCLUSIONS

A fatigue crack propagation problem was studied in this work and the algorithm developed has provided good results when compared to those obtained with the experimental tests. The problem exhibits a mixed-mode behavior and the crack propagation path was predicted very well through the MSED criterion. Applying the features of this criterion, the crack increment size was evaluated and, the total crack length predicted is in good agreement with the experimental observations. The fatigue life was modeled satisfactorily applying the concept of crack closure in the Paris law modified according to the Elber´s model with a different value of U than that predicted by this model. Further investigation is necessary to verify if the problem of crack closure is actuating combined with other mechanisms.

6. ACKNOWLEDGEMENTS

The authors would like to acknowledge the CNPq (The National Council for Scientific and Technological Development, Brazil), AFOSR (Air Force Office of Scientific Research, USA) and FAPESP (The State of São Paulo Research Foundation) for the financial support for this work.

7. REFERENCES

Aliabadi, M., 2002, "The Boundary Element Method: Applications in Solids and Structures", vol 2. John Wiley & Sons.
Brebbia, C. and Dominguez, J., 1992, "Boundary Elements: An Introductory Course", Wit Press Computational Mechanics Publications.
Bui, H., 1983, "Associated path independent j-integrals for separating mixed modes", Journal of Mechanics & Physics Solids, 31(6), pp. 439–448.
Cisilino, A. and Aliabadi, M., 2004, "Dual boundary element assessment of three-dimensional fatigue crack growth", Engineering Analysis with Boundary Elements, 28, pp. 1157–1173.
Elber, W., 1970, "Fatigue crack closure under cyclic tension", Engineering Fracture Mechanics, 2(1), pp. 37–44.
Elber, W., 1971, "The significance of fatigue crack closure", Damage Tolerance in Aircraft Structures ASTM STP 486, 486, pp. 230–242.
Elber, W., 1976, "Equivalent constant-amplitude concept for crack growth under spectrum loading", Fatigue Crack Growth Under Spectrum Loads ASTM STP, 595, pp. 236–250.
Meggiolaro, M. and Castro, J., 2001, "An evaluation of elber-type crack retardation models", In SAE (Ed.), II Seminário Internacional de Fadiga (SAE-Brasil), pp. 207–216.
Paris, P. and Erdogan, F., 1960, "A critical analysis of crack propagation laws", Journal of Basic Engineering Failure Analysis, 85, pp. 528–534.
Portela, A., 1992a, "Dual Boundary Element Incremental Analysis of Crack Growth", PhD thesis, Wessex Institute of Technology.
Portela, A., Aliabadi, M., and Rooke, D., 1992b, "The dual boundary element method: Efficient implementation for cracked problems", International Journal for Numerical Methods in Engineering, 33, pp. 1269–1287.
Rice, J., 1968, "A path independent integral and the approximate analysis of strain concentration by notches and cracks", Journal of Applied Mechanics, 35, pp. 379–386.
Sabelkin, V., Mall, S. and Avram, J., 2006, "Fatigue crack growth analysis of stiffened cracked panel repaired with bonded composite patch", Engineering Fracture Mechanics, (73), pp. 1553–1567.
Sato, M., 2009, "Modelagem de Problemas da Mecânica da Fratura e Propagação de Trincas em Fadiga", Master Dissertation, State University of Campinas, in Portuguese (in progress)
Sih, G., 1973a, "Energy-density concept in fracture mechanics", Engineering Fracture Mechanics, 5(4), pp. 1037 – 1040.
Sih, G., 1973b, "Some basic problems in fracture mechanics and new concepts", Engineering Fracture Mechanics, 5(4), pp. 1037–1040.

8. RESPONSABILITY NOTICE

The authors are the only responsible for the printed material included in this paper.